

# RoboAct-CLIP: Video-Driven Pre-training of Atomic Action Understanding for Robotics

Zhiyuan Zhang<sup>1</sup>, Yuxin He<sup>1</sup>, Yong Sun<sup>1</sup>, Junyu Shi<sup>1</sup>, Lijiang Liu<sup>1</sup>, Qiang Nie<sup>1,†</sup>

**Abstract**—Visual Language Models (VLMs) have emerged as pivotal tools for robotic systems, enabling cross-task generalization, dynamic environmental interaction, and long-horizon planning through multimodal perception and semantic reasoning. However, existing open-source VLMs predominantly trained for generic vision-language alignment tasks fail to model temporally correlated action semantics that are crucial for robotic manipulation effectively. While current image-based fine-tuning methods partially adapt VLMs to robotic applications, they fundamentally disregard temporal evolution patterns in video sequences and suffer from visual feature entanglement between robotic agents, manipulated objects, and environmental contexts, thereby limiting semantic decoupling capability for atomic actions and compromising model generalizability. To overcome these challenges, this work presents RoboAct-CLIP with dual technical contributions: 1) A dataset reconstruction framework that performs semantic-constrained action unit segmentation and re-annotation on open-source robotic videos, constructing purified training sets containing singular atomic actions (e.g., "grasp"); 2) A temporal-decoupling fine-tuning strategy based on Contrastive Language-Image Pretraining (CLIP) architecture, which disentangles temporal action features across video frames from object-centric characteristics to achieve hierarchical representation learning of robotic atomic actions. Experimental results in simulated environments demonstrate that the RoboAct-CLIP pretrained model achieves a 12% higher success rate than baseline VLMs, along with superior generalization in multi-object manipulation tasks. Cross-platform validation on physical robotic arms confirms the method's capability for stable atomic action execution. The proposed framework advances robotic action semantics understanding by effectively resolving temporal feature entanglement while providing a systematic paradigm for adapting VLMs to temporally sensitive robotic applications.

## I. INTRODUCTION

Recently, the application of Vision-Language Models (VLMs) in robotics has garnered significant attention, with their multimodal integration capabilities driving revolutionary advancements in robotic perception, decision-making, and control paradigms [1], [2], [3]. By establishing deep alignment between visual representations and linguistic semantics, VLMs demonstrate exceptional proficiency in interpreting complex environmental scenarios while achieving task generalization through natural language instructions. Notable breakthroughs include RT-2 [4], which pioneered the extension of VLMs into Vision-Language-Action (VLA) models through an end-to-end architecture for direct robotic action generation; RoboFlamingo [5], an open-source VLM-

based framework enabling zero-shot cross-scenario generalization with minimal demonstration data; and SpatialVLM [6], which enhances spatial reasoning capabilities to support 3D environment comprehension and dense reward annotation. The integration of closed-loop feedback systems [7] and atomic action decomposition methodologies [8] has further enhanced the practical utility of VLMs in dynamic task execution. These collective advancements signify that VLM-based robotic systems are progressively transcending the limitations of conventional approaches in semantic understanding and generalization capabilities, thereby establishing crucial groundwork for the development of universal intelligent agents.

Although VLMs have demonstrated potential in robotic applications, their training paradigms exhibit notable limitations. Current mainstream VLMs (e.g., CLIP[9], OpenFlamingo[10]) predominantly rely on static image-text pairs with minimal incorporation of robotic domain data, resulting in inadequate capture of temporal dynamics in continuous actions. While some studies attempt domain-specific fine-tuning using robotic data[11], [12] - exemplified by Robotic-CLIP[12]'s contrastive learning approach that incorporates action initiation and completion frames to enhance action outcome understanding - their implicit modeling of action processes through dual-frame comparisons fails to decode intermediate state transitions in continuous operations, such as trajectory optimization during grasping or fluid dynamic adjustments in pouring tasks. Similarly, RT-2[4] achieves end-to-end control through discretizing actions into text tokens, yet its joint training paradigm employing hybrid static image and robotic data inputs lacks explicit modeling of temporal features in video sequences. The neglect of temporal information may lead to two critical issues: first, models struggle to distinguish between action intentions and transient states (e.g., sequential "moving cup" versus "tilting cup" actions); second, cumulative errors in long-horizon tasks can cause policy trajectories to deviate significantly from expected paths[13], [14], [15]. These deficiencies reveal that current fine-tuning paradigms relying on static or sparsely sampled temporal data remain insufficient to meet the spatiotemporal modeling precision required for robotic atomic action understanding.

Furthermore, the visual features of the robot itself, manipulated objects, and background environment are highly entangled in video data, which exacerbates the difficulty of semantic decoupling for atomic actions. In complex operational scenarios (such as kitchen-based tableware organization), the motion trajectories of robotic arms, morphological changes

<sup>1</sup>ROAS Thrust, System Hub, Hong Kong University of Science and Technology (Guangzhou), Guangdong, China.

<sup>†</sup>Corresponding author. qiangnie@hkust-gz.edu.cn

in target objects (such as fluid dynamics during pouring), and background clutter (such as scattered items on tabletops) often create interfering visual features, making it challenging for models to distinguish between action subjects and contextual noise. This visual feature uncertainty tends to amplify hallucination phenomena in VLMs, thereby affecting the alignment between visual inputs and textual instructions, and consequently impacting overall model performance[16], [17]. To address this issue, approaches such as DP3[18] construct more efficient and complex visual representation modules to obtain more accurate visual features, while ACP[19] dynamically adjusts prediction intervals based on real-time data and integrates long-term memory. This methodology enables robots to recognize their limitations and seek human assistance when necessary. The integration of long-term memory within the ACP framework allows robots to learn from past experiences and continuously refine their decision-making processes. OmniManip[20], based on object-centered 3D interaction primitives, transforms the high-level reasoning capabilities of VLMs into low-level, high-precision robotic actions through a dual-loop system design incorporating VLM planning and robotic execution to mitigate related hallucination issues. However, existing methods still rely on manually defined complex network architectures and lack the ability to autonomously discover semantic boundaries of atomic actions from video sequences, which limits the adaptability of VLM models in open-world scenarios.

To address the aforementioned challenges, we present RoboAct-CLIP, a video pre-training model specifically designed for robotic atomic action understanding. Unlike existing approaches, our core innovation lies in the design of a Temporal Diff-Transformer module that enhances the model’s ability to extract and comprehend temporal features of atomic actions in videos, coupled with a feature disentanglement architecture that explicitly separates robotic embodiment features, action semantic features, and object manipulation features. Through three recombination modules utilizing Compositional CLIP Loss to align recombined features with reconstructed textual instructions, we further enhance the disentanglement effect. As illustrated in Figure 1, our model captures fine-grained temporal action information through frame differencing and temporal Transformer mechanisms, while the disentanglement module maintains low similarity between feature branches, thereby achieving purer action representations. This disentangled design enables the model to focus on the action itself, unaffected by environmental changes or object appearance variations. To support model training, we developed a semantically-guided data filtering and re-annotation methodology, screening video datasets into atomic action units and re-annotating them to ensure each training sample contains only a single, well-defined action semantic. Experimental results demonstrate that our approach significantly outperforms baseline models in robotic policy learning tasks and exhibits superior performance in multi-task generalization tests.

Our main contributions are as follows:

- We propose a novel framework, RoboAct-CLIP, that

enables robots to understand the essence of atomic actions through temporal-aware feature decoupling. To support this framework, we develop a comprehensive atomic action video filtering and re-annotation paradigm that provides high-quality training data.

- We design a temporal modeling method based on frame differencing and Transformer architecture, effectively capturing temporal action features in action videos
- We introduce a novel action feature disentanglement architecture, achieving pure representation learning of robotic actions through cosine similarity minimization and L2 regularization
- We validate the effectiveness of our model through simulation and physical robot experiments, demonstrating its potential in practical applications

## II. METHODOLOGY

In this section, we present the methodological framework for training RoboAct-CLIP. Our approach initiates with the establishment of a comprehensive curation and annotation pipeline based on open-source robotic video datasets. Subsequently, we architect RoboAct-CLIP through the systematic integration of two novel components: a Temporal Difference Transformer module for temporal reasoning and a Feature Disentanglement module for representation decoupling. The implementation paradigm for applying this architecture to robotic policy learning is then formally elaborated, demonstrating its operationalization in sequential decision-making tasks.

### A. Dataset Preparation

Here, we have selected the RH20T[21] dataset, an open-source collection. The RH20T dataset encompasses over 110,000 contact-rich robot manipulation sequences, spanning a variety of actions, environments, robots, and camera viewpoints. Additionally, the dataset provides corresponding human demonstration videos and language descriptions for each robotic sequence. Algorithm 1 illustrates our data preparation process:

As shown in Table I, after processing, the dataset consists of 199,797 videos categorized into 143 unique tasks. These videos encompass 52 different atomic actions and contain a total of 63,922,209 frames.

TABLE I  
SUMMARY OF THE PROCESSED RH20T DATASET

Item	Count
Total Videos	199,797
Unique Tasks	143
Distinct Atomic Actions	52
Total Frames	63,922,209

### B. RoboAct-CLIP

Our model extends the CLIP architecture by incorporating a temporal difference Transformer and feature disentanglement modules to achieve fine-grained understanding of robot manipulation actions. The core architecture is illustrated in Figure 1.

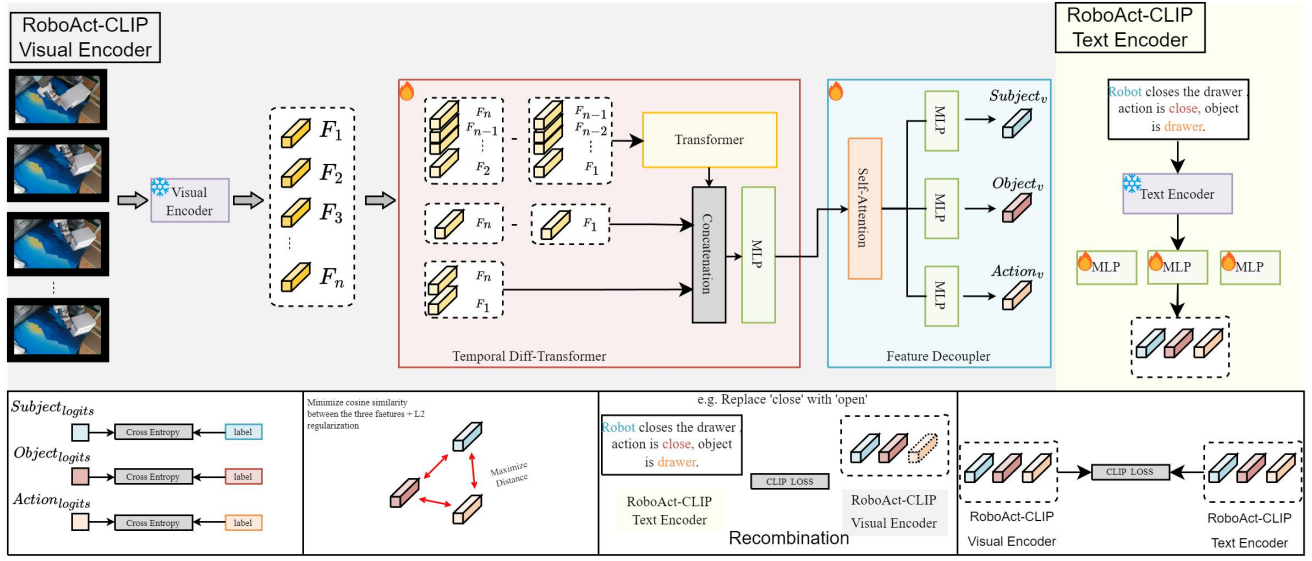


Fig. 1. Overall framework of RoboAct-CLIP.

#### Algorithm 1 Process Video Annotations

```

1: procedure DATASET PREPARATION
2:   Unzip dataset containing video files and their corresponding textual annotations.
3:   for each video file  $V$  in the dataset do
4:     Read the textual annotation  $T$  associated with  $V$ .
5:     Query the DeepSeek R1[22] API with  $T$  using the prompt: "Please identify how many actions are described in the following text, along with the relevant verbs and objects."
6:     if the response indicates multiple actions then
7:       Eliminate  $V$  from further consideration.
8:     else
9:       Extract subject ( $S$ ), action ( $A$ ), and object ( $O$ ) information from the API response.
10:      Generate description as "Robot (or Human) [ $A$ ] [ $O$ ], Action is  $A$ , Object is  $O$ ."
11:    end if
12:  end for
13: end procedure

```

1) *CLIP Text Encoder*: The text encoder processes natural language instructions  $I_{\text{text}}$  and aligns them with visual representations through our multi-branch architecture:

$$F_{\text{text}} = \text{CLIP}_{\text{text}}(\text{tokenize}(I_{\text{text}})) \quad (1)$$

We decompose the text representation into three semantic components:

$$\begin{aligned} F_{\text{text-subject}} &= \text{MLP}_{\text{text-subject}}(F_{\text{text}}), \\ F_{\text{text-action}} &= \text{MLP}_{\text{text-action}}(F_{\text{text}}), \\ F_{\text{text-object}} &= \text{MLP}_{\text{text-object}}(F_{\text{text}}) \end{aligned} \quad (2)$$

2) *CLIP Visual Encoder*: Specifically, each video in our processed dataset consists of a sequence of frames

$[Frame_{\text{start}}, \dots, Frame_i, \dots, Frame_{\text{end}}]$ , where  $Frame_i \in \mathbb{R}^{H \times W \times 4}$ . We first uniformly sample  $n$  frames from each video where  $n$  is 16 in our case, then process each frame individually through a frozen CLIP visual encoder to obtain corresponding visual representations:

$$F_i = \text{CLIP}_{\text{VisualEncoder}}(Frame_i) \quad (3)$$

This results in a sequence of frame features  $[F_1, \dots, F_i, \dots, F_n]$ .

3) *Temporal Diff-Transformer*: After obtaining the frame-level features  $\{F_i\}_{i=1}^n$  and  $F_i \in \mathbb{R}^d$  ( $d$  is the embedding dimension), we employ a sophisticated temporal modeling approach to capture the dynamic information in the video sequence. We first compute the consecutive frame differences to capture the temporal dynamics:

$$\Delta F_i = F_i - F_{i-1}, \quad i \in \{2, \dots, n\} \quad (4)$$

The differential operation between adjacent frame embeddings functions as an implicit attention mechanism that suppresses static environmental context and extraneous visual elements, thereby accentuating the temporal action dynamics. This feature difference approach effectively isolates the salient motion patterns by computing the gradient of visual representations across the temporal dimension, resulting in a more discriminative signal for action recognition tasks.

The sequence of enhanced difference features  $\{\Delta F_i\}_{i=2}^n$  is then processed through a Transformer[23] encoder with relative positional encoding to model the higher-order temporal relationships:

$$\{Tem_i\}_{i=2}^n = \text{Transformer}(\{\Delta F_i\}_{i=2}^n) \quad (5)$$

We extract the last output from the Transformer sequence, which encodes the cumulative temporal information:

$$Tem = \Delta Tem_n \quad (6)$$

In parallel, we compute the difference between the last and first frames to capture the overall effect of the action in the video:

$$\Delta F = F_n - F_1 \quad (7)$$

Finally, we concatenate the Transformer output  $Temp$  and the start-end difference feature  $\Delta F$ , the start and end frame  $F_1, F_n$ , followed by a multi-layer perceptron (MLP) projection to obtain the final visual representation:

$$F_v = \text{MLP}(\text{Concat}[Temp; \Delta F; F_1; T_n]) \quad (8)$$

4) *Feature Disentanglement*: After obtaining the fused visual representation  $F_v$ , we employ a novel feature disentanglement module to decompose it into 3 semantically meaningful components corresponding to different aspects of the robot manipulation task. To enhance the feature’s contextual awareness, we apply a self-attention mechanism:

$$F_{\text{attn}} = \text{MultiHeadAttention}(Q = F_v, K = F_v, V = F_v) \quad (9)$$

Then the attention-enhanced representation is projected into three separate semantic spaces:

$$\begin{aligned} F_{\text{subject}} &= \text{MLP}_{\text{subject}}(F_{\text{attn}}) \\ F_{\text{object}} &= \text{MLP}_{\text{object}}(F_{\text{attn}}) \\ F_{\text{action}} &= \text{MLP}_{\text{action}}(F_{\text{attn}}) \end{aligned} \quad (10)$$

To ensure effective separation of the 3 components, we apply an orthogonality constraint that minimizes the cosine similarity between the branch features:

$$\begin{aligned} \mathcal{L}_{\text{sim}} = -\frac{1}{N} \sum_{i=1}^N \frac{1}{3} & (\text{CosSim}(F_{\text{subject}}, F_{\text{action}}) + \\ & \text{CosSim}(F_{\text{subject}}, F_{\text{object}}) + \\ & \text{CosSim}(F_{\text{action}}, F_{\text{object}})) \end{aligned} \quad (11)$$

where  $\text{CosSim}(a, b) = \frac{a \cdot b}{\|a\| \cdot \|b\|}$  is the cosine similarity, and  $N$  is the batch size.

Additionally, we apply an L2 regularization to prevent feature magnitude explosion:

$$\mathcal{L}_{\text{L2}} = 0.01 \cdot (\|F_{\text{subject}}\|_2 + \|F_{\text{action}}\|_2 + \|F_{\text{object}}\|_2) \quad (12)$$

To further enhance the performance of our disentanglement module, we implement a feature bank mechanism that stores representative features for each category of subject, action, and object:

$$\mathcal{B}_{\text{subject}} = \{F_{\text{subject}}^1, F_{\text{subject}}^2, \dots, F_{\text{subject}}^{K_s}\} \quad (13)$$

$$\mathcal{B}_{\text{action}} = \{F_{\text{action}}^1, F_{\text{action}}^2, \dots, F_{\text{action}}^{K_a}\} \quad (14)$$

$$\mathcal{B}_{\text{object}} = \{F_{\text{object}}^1, F_{\text{object}}^2, \dots, F_{\text{object}}^{K_o}\} \quad (15)$$

where  $K_s$ ,  $K_a$ , and  $K_o$  represent the number of unique subjects, actions, and objects in our dataset. The feature banks are updated at fixed step intervals during training. Every  $N$  steps, we compute the average feature for each

class from the current batch and replace the corresponding entry in the feature bank:

$$\begin{aligned} & \text{if step} \bmod \text{Setting\_Step} = 0 : \\ & \mathcal{B}_{\text{subject}}[c] = F_{\text{subject}}^i \quad \text{where } i \text{ has class } c \end{aligned} \quad (16)$$

where  $\mathcal{S}_c$  is the set of samples with subject class  $c$  in the current batch. This direct replacement strategy is applied similarly for action and object feature banks. When multiple instances of the same class appear in a batch, we use the last instance’s feature for the update.

During the recombination phase, we leverage these stored features to compute an additional CLIP loss between recombined visual features and corresponding text instructions. For instance, the stored features for "robot" (subject), "open" (action), and "drawer" (object) can be recombined to create a synthetic visual representation that is then compared against the text encoding of "Robot opens the drawer, action is open." This approach allows us to evaluate whether the disentangled features can be effectively recombined to match novel combinations of subjects, actions, and objects described in text instructions:

$$F_{\text{recomb}}^{i,j,k} = \text{Combiner}(\mathcal{B}_{\text{subject}}[i], \mathcal{B}_{\text{action}}[j], \mathcal{B}_{\text{object}}[k]) \quad (17)$$

$$T^{i,j,k} = \text{RoboAct-CLIP-TextEncoder}(\text{" } i \text{ } j \text{ the } k, \text{ action is } j \text{"}) \quad (18)$$

$$\mathcal{L}_{\text{recomb}} = -\frac{1}{N} \sum_{i=1}^N \log \frac{\exp(\text{sim}(F_{\text{recomb}}^a, T^a)/\tau)}{\sum_{b \in \mathcal{M}} \exp(\text{sim}(F_{\text{recomb}}^a, T^b)/\tau)} \quad (19)$$

where  $\mathcal{M}$  is a set of valid (subject, action, object) triplets sampled from the feature banks, and for each sample  $a \in \mathcal{M}$  in the batch of size  $N$ , we randomly select one triplet from  $\mathcal{M}$ .

This recombination loss encourages the disentangled features to capture the essential characteristics of each semantic component, as they must be effectively recombined to match the corresponding text descriptions. The final disentanglement loss is thus enhanced:

$$\mathcal{L}_{\text{disent-enhanced}} = \lambda_{\text{ortho}} \cdot (\mathcal{L}_{\text{sim}} + \mathcal{L}_{\text{L2}}) + \lambda_{\text{recomb}} \mathcal{L}_{\text{recomb}} \quad (20)$$

where  $\lambda_{\text{ortho}}$  and  $\lambda_{\text{recomb}}$  are hyperparameters controlling the contribution of the losses.

To guide the learning process and enhance the model’s performance, we incorporate auxiliary classification tasks for each disentangled feature. These auxiliary tasks provide additional supervision signals that help the model learn more discriminative and semantically meaningful representations[24], [25]:

$$\begin{aligned} P_{\text{subject}} &= \text{Softmax}(\text{MLP}_{\text{classify-subject}}(F_{\text{attn}})) \\ P_{\text{object}} &= \text{Softmax}(\text{MLP}_{\text{classify-object}}(F_{\text{attn}})) \\ P_{\text{action}} &= \text{Softmax}(\text{MLP}_{\text{classify-action}}(F_{\text{attn}})) \end{aligned} \quad (21)$$

with the combined auxiliary classification loss:

$$\begin{aligned}\mathcal{L}_{\text{aux}} = & -\frac{1}{N} \sum_{i=1}^N \alpha_s \text{CE}(P_{\text{subject}}, y_{\text{subject}}) \\ & -\frac{1}{N} \sum_{i=1}^N \alpha_a \text{CE}(P_{\text{action}}, y_{\text{action}}) \\ & -\frac{1}{N} \sum_{i=1}^N \alpha_o \text{CE}(P_{\text{object}}, y_{\text{object}})\end{aligned}\quad (22)$$

where CE is the cross-entropy,  $\alpha_s$ ,  $\alpha_a$ ,  $\alpha_o$  are task-specific weights and  $y$  is the label. By incorporating these auxiliary tasks, we encourage each branch to focus on its specific semantic aspect, thereby improving the overall representation quality and downstream task performance.

This feature disentanglement approach enables our model to learn specialized representations for different aspects of manipulation videos, facilitating more effective downstream task performance and interpretability.

5) *Loss*: To ensure cross-modal alignment between visual and textual representations, we compute the final CLIP contrastive loss:

$$\begin{aligned}F_{\text{video}}^i &= \text{Concat}(F_{\text{subject}}^i, F_{\text{object}}^i, F_{\text{action}}^i) \\ F_{\text{text}}^i &= \text{Concat}(F_{\text{text.subject}}^i, F_{\text{text.object}}^i, F_{\text{text.action}}^i) \\ \mathcal{L}_{\text{CLIP}} &= -\frac{1}{N} \sum_{i=1}^N \log \frac{\exp(\text{sim}(F_{\text{video}}^i, F_{\text{text}}^i)/\tau)}{\sum_{j=1}^N \exp(\text{sim}(F_{\text{video}}^i, F_{\text{text}}^j)/\tau)}\end{aligned}\quad (23)$$

where  $\text{sim}(\cdot, \cdot)$  is the cosine similarity function, and  $\tau$  is the temperature parameter.

$$\mathcal{L}_{\text{Total}} = \mathcal{L}_{\text{CLIP}} + \lambda_{\text{disent}} * \mathcal{L}_{\text{disent-enhanced}} + \lambda_{\text{aux}} * \mathcal{L}_{\text{aux}} \quad (24)$$

where  $\lambda_{\text{disent}}$  and  $\lambda_{\text{aux}}$  are hyperparameters controlling the contribution of the losses.

### III. EXPERIMENTS

In this section, we conducted robotic tasks in simulated environments to demonstrate the effectiveness of our proposed RoboAct-CLIP. Specifically, we employed the pre-trained RoboAct-CLIP as an information encoder for downstream tasks, freezing the weights of this network component during the training process. Additionally, comprehensive ablation studies were performed to validate the efficacy of our designed Temporal Diff-Transformer and Feature Disentanglement modules. Finally, experiments with physical robotic manipulators in real-world settings further confirmed the effectiveness of our approach.

#### A. Simulation Experiment

To evaluate our RoboAct-CLIP model, we conducted experiments in the Franka Kitchen[26] simulation environment, a benchmark for robotic manipulation in household settings. This environment features interactive kitchen objects requiring precise manipulation and semantic understanding of instructions.

We employed a robotic arm to perform four representative tasks:

- Task 1: Opening the middle drawer of the cabinet
- Task 2: Pushing a plate to the front of the stove
- Task 3: Placing cream cheese in a bowl
- Task 4: Turning on the stove

As for the evaluation metrics, we reported the success rate, defined as the percentage of episodes where the robot successfully completed the instructed task within a maximum of 200 timesteps.

We compared our RoboAct-CLIP against several state-of-the-art baselines:

- **R3M**[27]: A ResNet50-based model pre-trained on visual data to obtain general visual representations for robotic tasks.
- **MPI**[28]: A model featuring a multimodal transformer encoder and a transformer decoder, designed to predict image-goal interaction states and detect interaction objects. We evaluated both ViT-small and ViT-Base versions.
- **CLIP**[9]: The original CLIP model without any fine-tuning, used as a feature encoder.
- **RoboAct-CLIP (Ours)**: Our proposed model with temporal modeling and feature disentanglement.

All methods were integrated into the same policy learning framework for fair comparison, with their respective encoders frozen during policy training.

Table II presents the performance comparison between our RoboAct-CLIP and the baseline methods across the manipulation tasks.

TABLE II  
SUCCESS RATES (%) ON FRANKA KITCHEN MANIPULATION TASKS

Method	Task 1	Task 2	Task 3	Task 4	Overall
R3M	46.0%	80.0%	58.0%	52.0%	59.0%
MPI (Small)	50.0%	74.0%	38.0%	66.0%	57.0%
MPI (Base)	62.0%	70.0%	44.0%	82.0%	64.5%
CLIP	86.0%	76.0%	22.0%	20.0%	51.0%
RoboAct-CLIP	90.0%	84.0%	56.0%	76.0%	76.5%

Our RoboAct-CLIP model significantly outperformed all baseline methods across all tasks, achieving an average success rate improvement of 12.0% compared to the best-performing baseline, MPI (Base). Further analysis indicates that the superior performance of our model can be attributed to two key factors: (1) The Temporal Diff-Transformer effectively captures the dynamic patterns of manipulation actions, enabling more precise action execution; and (2) The Feature Disentanglement module successfully separates robot embodiment features from action and object features, allowing the policy to focus on task-relevant information while maintaining robustness to environmental variations.

Figure 2 illustrates the execution process of our RoboAct-CLIP model on the four manipulation tasks. These visualizations demonstrate how our model effectively handles different types of interactions, from precise grasping and manipulation (opening drawers, turning knobs) to controlled

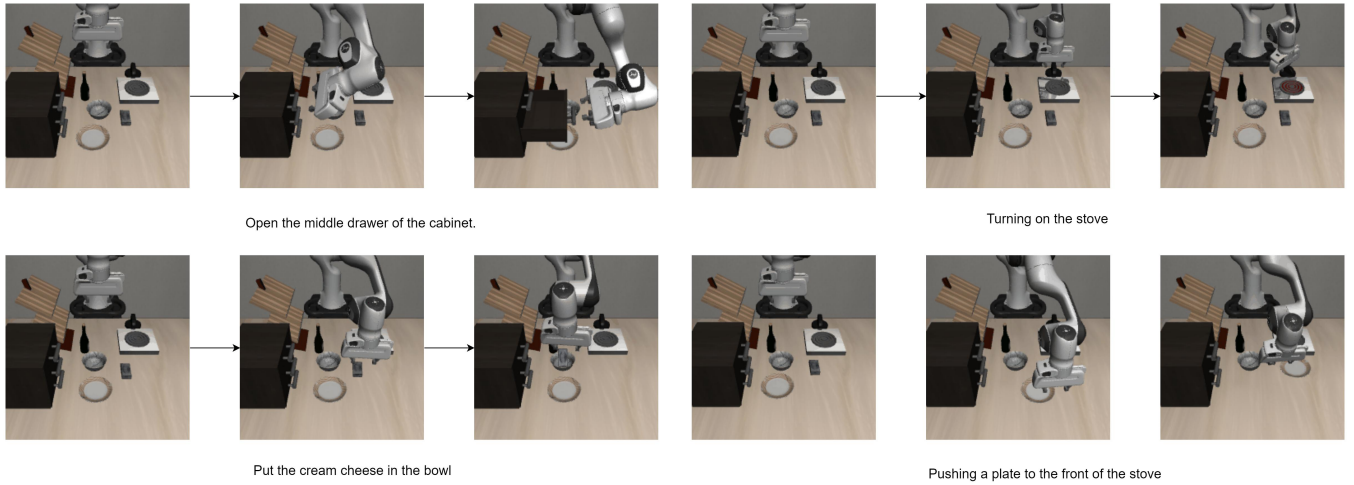


Fig. 2. Visualization of RoboAct-CLIP performing four manipulation tasks in the Franka Kitchen environment. Each row shows a different task. Our model demonstrates precise control throughout the action sequences, successfully completing diverse manipulation tasks requiring different interaction patterns.

pushing and placing of objects. These visualizations further substantiate our findings, validating the exceptional performance of the RoboAct-CLIP model as a feature encoder. The qualitative results demonstrate the model’s capacity to generate precise and contextually appropriate representations that facilitate successful task completion across diverse manipulation scenarios.

### B. Ablation Study

TABLE III  
SUCCESS RATES (%) ON ABLATION STUDIES ACROSS MANIPULATION TASKS

Method	Task 1	Task 2	Task 3	Task 4	Overall
Ablation 1	78.0%	72.0%	70.0%	44.0%	66.0%
Ablation 2	88.0%	76.0%	56.0%	60.0%	70.0%
RoboAct-CLIP	90.0%	84.0%	56.0%	76.0%	76.5%

To further investigate the impact of the Temporal Diff-Transformer module and Feature Disentanglement module on model performance, we conducted the following ablation experiments:

- 1) **Ablation 1: Without Temporal Diff-Transformer** - In this configuration, the input to equation 8 includes only  $F_1$  and  $F_n$ , eliminating the temporal modeling capabilities to assess this module’s contribution to overall performance.
- 2) **Ablation 2: Without Feature Disentanglement** - Here, we removed the Feature Disentanglement component, using only the output from equation 8 as the final representation from the RoboAct-CLIP Visual Encoder, which is then aligned with text features during training.

The ablation results clearly demonstrate the importance of both proposed components. Removing the Temporal Diff-Transformer (Ablation 1) led to a significant performance drop of 10.5 percentage points in overall success rate,

with particularly pronounced effects on Tasks 2 and 4. This confirms the critical role of temporal modeling in capturing action dynamics. Similarly, the absence of the Feature Disentanglement module (Ablation 2) resulted in a 6.5 percentage point decrease in overall performance, highlighting its effectiveness in separating task-relevant features from embodiment-specific information. These findings validate our architectural design choices and underscore the complementary nature of the proposed components.

### C. Robotic Experiment

To further validate the efficacy of RoboAct-CLIP, we conducted experiments in real-world environments. We maintained the same network architecture as in the simulation experiments while training the policy on a dataset collected through teleoperation. The sequential manipulation task consisted of the following steps:

- 1) Open the middle drawer
- 2) Pick up the scotch tape
- 3) Place the scotch tape on the table
- 4) Close the drawer

Figure 3 illustrates the execution sequence of these actions. The robot successfully completed this complex manipulation sequence, demonstrating the transferability of our approach from simulation to real-world scenarios. The temporal modeling capabilities of our Temporal Diff-Transformer proved particularly valuable in handling the variations in lighting, object appearance, and robot dynamics present in real-world settings.

## IV. CONCLUSIONS

This paper presented RoboAct-CLIP, a novel approach that enhances Vision-Language Models for atomic action understanding for robotics through temporal-aware feature decoupling. Our Temporal Diff-Transformer effectively captures action dynamics while the Feature Disentanglement module

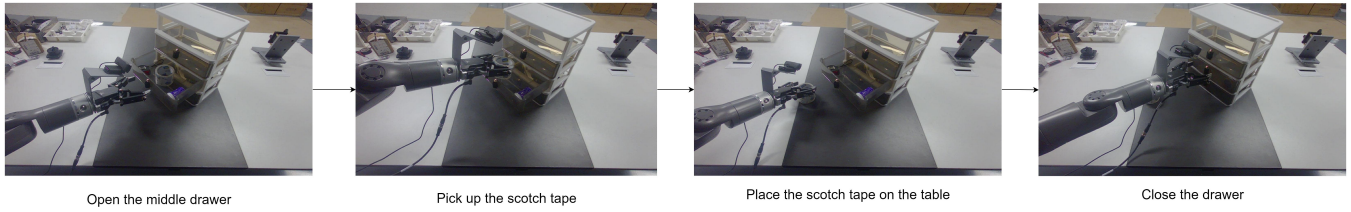


Fig. 3. Execution sequence of the real-world manipulation task using RoboAct-CLIP.

separates subject, action, and object representations, addressing key limitations in existing VLMs for robotic applications. Experimental results demonstrate RoboAct-CLIP’s superior performance, achieving a 12% higher success rate than baseline methods across various manipulation tasks in both simulated and real-world environments. Ablation studies confirm the critical contribution of each proposed component. By resolving temporal feature entanglement, our approach advances robotic action understanding and provides a systematic framework for adapting VLMs to manipulation tasks guided by natural language instructions.

#### REFERENCES

- [1] P. Li, Z. An, S. Abrar, and L. Zhou, “Large language models for multi-robot systems: A survey,” 2025.
- [2] H. Jeong, H. Lee, C. Kim, and S. Shin, “A survey of robot intelligence with large language models,” *Applied Sciences*, vol. 14, no. 19, p. 8868, 2024.
- [3] Y. Ma, Z. Song, Y. Zhuang, J. Hao, and I. King, “A survey on vision-language-action models for embodied ai,” *arXiv preprint arXiv:2405.14093*, 2024.
- [4] A. Brohan, N. Brown, J. Carbajal, Y. Chebotar, X. Chen, K. Chormanski, T. Ding, D. Driess, A. Dubey, C. Finn, *et al.*, “Rt-2: Vision-language-action models transfer web knowledge to robotic control,” *arXiv preprint arXiv:2307.15818*, 2023.
- [5] X. Li, M. Liu, H. Zhang, C. Yu, J. Xu, H. Wu, C. Cheang, Y. Jing, W. Zhang, H. Liu, H. Li, and T. Kong, “Vision-language foundation models as effective robot imitators,” *arXiv preprint arXiv:2311.01378*, 2023.
- [6] B. Chen, Z. Xu, S. Kirmani, B. Ichter, D. Driess, P. Florence, D. Sadigh, L. Guibas, and F. Xia, “Spatialvlm: Endowing vision-language models with spatial reasoning capabilities,” 2024.
- [7] P. Zhi, Z. Zhang, M. Han, Z. Zhang, Z. Li, Z. Jiao, B. Jia, and S. Huang, “Closed-loop open-vocabulary mobile manipulation with gpt-4v,” 2024.
- [8] Y. Wang, R. Xiao, J. Y. L. Kasahara, R. Yajima, K. Nagatani, A. Yamashita, and H. Asama, “Dart-llm: Dependency-aware multi-robot task decomposition and execution using large language models,” *arXiv preprint arXiv:2411.09022*, 2024.
- [9] A. Radford, J. W. Kim, C. Hallacy, A. Ramesh, G. Goh, S. Agarwal, G. Sastry, A. Askell, P. Mishkin, J. Clark, *et al.*, “Learning transferable visual models from natural language supervision,” in *International conference on machine learning*, pp. 8748–8763, PmLR, 2021.
- [10] A. Awadalla, I. Gao, J. Gardner, J. Hessel, Y. Hanafy, W. Zhu, K. Marathe, Y. Bitton, S. Gadre, S. Sagawa, *et al.*, “Openflamingo: An open-source framework for training large autoregressive vision-language models,” *arXiv preprint arXiv:2308.01390*, 2023.
- [11] S. Karamcheti, S. Nair, A. S. Chen, T. Kollar, C. Finn, D. Sadigh, and P. Liang, “Language-driven representation learning for robotics,” *arXiv preprint arXiv:2302.12766*, 2023.
- [12] N. Nguyen, M. N. Vu, T. D. Ta, B. Huang, T. Vo, N. Le, and A. Nguyen, “Robotic-clip: Fine-tuning clip on action data for robotic applications,” *arXiv preprint arXiv:2409.17727*, 2024.
- [13] M. Kim, K. Pertsch, S. Karamcheti, T. Xiao, A. Balakrishna, S. Nair, R. Rafailov, E. Foster, G. Lam, P. Sanketi, Q. Vuong, T. Kollar, B. Burchfiel, R. Tedrake, D. Sadigh, S. Levine, P. Liang, and C. Finn, “Openvla: An open-source vision-language-action model,” *arXiv preprint arXiv:2406.09246*, 2024.
- [14] M. Pan, J. Zhang, T. Wu, Y. Zhao, W. Gao, and H. Dong, “Omnimanip: Towards general robotic manipulation via object-centric interaction primitives as spatial constraints,” 2025.
- [15] O. Mees, L. Hermann, E. Rosete-Beas, and W. Burgard, “Calvin: A benchmark for language-conditioned policy learning for long-horizon robot manipulation tasks,” *IEEE Robotics and Automation Letters*, vol. 7, no. 3, pp. 7327–7334, 2022.
- [16] H. Liu, W. Xue, Y. Chen, D. Chen, X. Zhao, K. Wang, L. Hou, R. Li, and W. Peng, “A survey on hallucination in large vision-language models,” *arXiv preprint arXiv:2402.00253*, 2024.
- [17] N. Chakraborty, M. Ornik, and K. Driggs-Campbell, “Hallucination detection in foundation models for decision-making: A flexible definition and review of the state of the art,” *ACM Computing Surveys*, 2025.
- [18] Y. Ze, G. Zhang, K. Zhang, C. Hu, M. Wang, and H. Xu, “3d diffusion policy: Generalizable visuomotor policy learning via simple 3d representations,” 2024.
- [19] A. Mistic, “Robots that adaptively learn when to ask for help: Hallucination reduction in robotic task planning using large language models,” Master’s thesis, NTNU, 2024.
- [20] M. Pan, J. Zhang, T. Wu, Y. Zhao, W. Gao, and H. Dong, “Omnimanip: Towards general robotic manipulation via object-centric interaction primitives as spatial constraints,” *arXiv preprint arXiv:2501.03841*, 2025.
- [21] H.-S. Fang, H. Fang, Z. Tang, J. Liu, C. Wang, J. Wang, H. Zhu, and C. Lu, “Rh20t: A comprehensive robotic dataset for learning diverse skills in one-shot,” in *2024 IEEE International Conference on Robotics and Automation (ICRA)*, pp. 653–660, IEEE, 2024.
- [22] D. Guo, D. Yang, H. Zhang, J. Song, R. Zhang, R. Xu, Q. Zhu, S. Ma, P. Wang, X. Bi, *et al.*, “Deepseek-r1: Incentivizing reasoning capability in llms via reinforcement learning,” *arXiv preprint arXiv:2501.12948*, 2025.
- [23] A. Vaswani, N. Shazeer, N. Parmar, J. Uszkoreit, L. Jones, A. N. Gomez, Ł. Kaiser, and I. Polosukhin, “Attention is all you need,” *Advances in neural information processing systems*, vol. 30, 2017.
- [24] Z. Zhang, Q. Zhang, X. Wu, X. Shi, G. Liao, Y. Wang, X. Wang, and D. Zhao, “User response modeling in reinforcement learning for ads allocation,” in *Companion Proceedings of the ACM Web Conference 2024, WWW ’24*, (New York, NY, USA), p. 131–140, Association for Computing Machinery, 2024.
- [25] Z. Wang, G. Liao, X. Shi, X. Wu, C. Zhang, Y. Wang, X. Wang, and D. Wang, “Learning list-wise representation in reinforcement learning for ads allocation with multiple auxiliary tasks,” in *Proceedings of the 31st ACM International Conference on Information & Knowledge Management, CIKM ’22*, (New York, NY, USA), p. 3555–3564, Association for Computing Machinery, 2022.
- [26] A. Gupta, V. Kumar, C. Lynch, S. Levine, and K. Hausman, “Relay policy learning: Solving long-horizon tasks via imitation and reinforcement learning,” *arXiv preprint arXiv:1910.11956*, 2019.
- [27] S. Nair, A. Rajeswaran, V. Kumar, C. Finn, and A. Gupta, “R3m: A universal visual representation for robot manipulation,” *arXiv preprint arXiv:2203.12601*, 2022.
- [28] J. Zeng, Q. Bu, B. Wang, W. Xia, L. Chen, H. Dong, H. Song, D. Wang, D. Hu, P. Luo, *et al.*, “Learning manipulation by predicting interaction,” *arXiv preprint arXiv:2406.00439*, 2024.